

# Minocycline and Diacetyl Minocycline Eye Drops Reduce Ocular Neovascularization in Mice

Joshua O. Willms<sup>1,\*</sup>, Kelly Mitchell<sup>2,\*</sup>, Mayank Shashtri<sup>3</sup>, Olof Sundin<sup>2</sup>, Xiaobo Liu<sup>1</sup>, Praneetha Panthagani<sup>1</sup>, Phat Tran<sup>2</sup>, Stephany Navarro<sup>4</sup>, Colton Sniegowski<sup>4</sup>, Abdul A. Shaik<sup>4</sup>, Tristin Chaudhury<sup>1</sup>, Ted W. Reid<sup>2</sup>, and Susan E. Bergeson<sup>4</sup>

<sup>1</sup> Department of Pharmacology and Neuroscience, Texas Tech University Health Sciences Center, Lubbock, TX, USA

<sup>2</sup> Department of Ophthalmology and Visual Sciences, Texas Tech University Health Sciences Center, Lubbock, TX, USA

<sup>3</sup> AttachChem, Lubbock, TX, USA

<sup>4</sup> Department of Cell Biology and Biochemistry, Texas Tech University Health Sciences Center, Lubbock, TX, USA

**Correspondence:** Susan E. Bergeson, 3601 4th St, MS6540, Lubbock, TX 79430, USA. e-mail:

[susan.bergeson@ttuhsc.edu](mailto:susan.bergeson@ttuhsc.edu)

Ted W. Reid, 3601 4th St, MS7217, Lubbock, TX 79430, USA. e-mail:

[ted.reid@ttuhsc.edu](mailto:ted.reid@ttuhsc.edu)

**Received:** November 7, 2022

**Accepted:** September 24, 2023

**Published:** December 8, 2023

**Keywords:** choroidal neovascularization; ocular angiogenesis; minocycline; tetracyclines; eye drop

**Citation:** Willms JO, Mitchell K, Shashtri M, Sundin O, Liu X, Panthagani P, Tran P, Navarro S, Sniegowski C, Shaik AA, Chaudhury T, Reid TW, Bergeson SE. Minocycline and diacetyl minocycline eye drops reduce ocular neovascularization in mice. *Transl Vis Sci Technol*. 2023;12(12):10,

<https://doi.org/10.1167/tvst.12.12.10>

<https://doi.org/10.1167/tvst.12.12.10>

**Purpose:** To evaluate the efficacy of minocycline and a novel, modified minocycline analogue that lacks antimicrobial action, diacetyl minocycline (DAM), on choroidal neovascularization (CNV) in mice of both sexes.

**Methods:** CNV was induced via laser injury in female and male C57BL/6J mice. Minocycline, DAM, or saline was administered via topical eye drops twice a day for 2 weeks starting the day after laser injury. CNV volume was measured using immunohistochemistry labeling and confocal microscopy.

**Results:** Minocycline reduced lesion volume by 79% ( $P \leq 0.0004$ ) in female and male mice. DAM reduced lesion volume by 73% ( $P \leq 0.001$ ) in female and male mice. There was no significant difference in lesion volume between minocycline and DAM treatment groups or between female and male mice.

**Conclusions:** Both minocycline and DAM eye drops significantly reduced laser-induced CNV lesion volume in female and male mice. While oral tetracyclines have been shown to mitigate pathologic neovascularization in both preclinical studies and clinical trials, the present data are the first to suggest that tetracycline derivatives may be effective to reduce pathologic CNV when administered via topical eye drops. However, the action is unrelated to antimicrobial action. Targeted delivery of these medications via eye drops may reduce the potential for systemic side effects.

**Translational Relevance:** Topical administration of minocycline and/or DAM via eye drops may represent a novel therapeutic strategy for disorders involving pathologic CNV.

## Introduction

Pathologic choroidal neovascularization (CNV) is a major contributor to vision loss. CNV contributes to the pathogenesis of potentially debilitating ocular disorders, such as macular degeneration.<sup>1–3</sup> In age-related macular degeneration (AMD), patients can develop rapid vision loss due to compromise of Bruch's membrane, increased expression of vascular endothelial growth factor (VEGF), and vascular invasion

from the choroid into the retinal pigment epithelium (RPE) and subretinal space.<sup>4–6</sup> Microglial activation and matrix metalloproteinases (MMPs) also play a role in disease progression.<sup>7–13</sup> Current therapies for CNV-related disorders include intravitreal anti-VEGF injections (e.g., ranibizumab, aflibercept) and photodynamic therapy.<sup>14–17</sup> While intravitreal anti-VEGF injections are effective to treat CNV-related disorders, they may increase risk for systemic vascular events (e.g., cerebrovascular accidents, nonocular hemorrhage) and require frequent, expensive, uncomfortable injections

into the eye.<sup>15,18</sup> The treatment involves intraocular injections, which have a low but nonzero risk of serious adverse effects (e.g., endophthalmitis). Accordingly, these injections are only administered by ophthalmologists specially trained to do so safely. Intravitreal shot administration can consume a large portion of an ophthalmologist's clinical time each day. Even when the injection goes well, patients describe the experience as generally unpleasant with the eye usually mildly irritated for 12 to 24 hours after each injection. A cohort study conducted in 2018 found that more than 20% of patients treated with intraocular anti-VEGF injections do not return for follow-up treatments.<sup>19</sup> Anti-VEGF medications range in cost from several hundred to several thousand dollars per injection and contribute a substantial burden to the US health care system: ranibizumab and aflibercept alone consume 12% of the annual Medicare Plan B budget.<sup>20</sup> Antioxidant/zinc supplementation is only effective for prevention or delay of age-related macular degeneration, not for treatment.<sup>15</sup> Based on these limitations, alternative treatment strategies are needed.

Minocycline is a tetracycline antibiotic with known immunomodulatory and antiangiogenic properties.<sup>21,22</sup> Minocycline has been shown to inhibit retinal neovascularization,<sup>23,24</sup> inhibit corneal neovascularization,<sup>25</sup> modulate microglial activity,<sup>24</sup> and suppress expression of MMPs and VEGF.<sup>21,22,26–28</sup> Minocycline and doxycycline (another tetracycline antibiotic) have shown promise in preclinical studies and clinical trials of CNV-related disorders.<sup>29–34</sup> Most notably, minocycline eye drops (1 mg/mL) were safe and effective in a rat model of diabetic retinopathy.<sup>35</sup> However, the antimicrobial action of minocycline can cause problematic side effects, contribute to antimicrobial resistance, and devastate microbiota, particularly with long-term use and systemic administration.<sup>26,36–38</sup> In this study, two hypotheses were tested to reduce potential side effects of minocycline: (1) targeted administration of minocycline via topical eye drops would be efficacious to treat CNV, and (2) modification of minocycline to remove the antimicrobial action, thereby generating a novel modified minocycline analogue, diacetyl minocycline (DAM; also delivered via eye drops), would treat CNV as well as minocycline. Both treatment strategies were tested in a model of CNV in female and male mice.

## Methods

### Animal Husbandry

All animals were treated in accordance with the Association for Research in Vision and Ophthalmol-

ogy Statement on the Use of Animals in Ophthalmic and Vision Research. All experimental protocols were conducted under the approval of the Texas Tech University Health Sciences Center Institutional Animal Care and Use Committee in our Association of Assessment and Accreditation of Laboratory Animal Care (AAALAC) accredited Laboratory Animal Resource Facility.

### Laser-Induced Choroidal Neovascularization

CNV was induced in male and female C57BL/6J mice (7–9 weeks old) via laser disruption of Bruch's membrane as previously described.<sup>39–41</sup> Briefly, pupils were dilated with topical 1% tropicamide and 2.5% phenylephrine (Alcon, Fort Worth, TX, USA), and mice were anesthetized with isoflurane (1.5–2% at 0.5 L/min) during ocular surgeries. The retina was visualized with an indirect ophthalmoscope using a 30-diopter lens. Bruch's membrane was disrupted via laser ablation by an individual masked to treatment groups using a Nd:YAG 532-nm laser (Alcon) adjusted to 80 to 90 mW with an exposure time of 0.100 seconds and a spot size of 50  $\mu$ m. Breakage of Bruch's membrane was verified with observation of bubble formation. Three to four laser shots were placed in both left and right eyes at approximately two disc diameters away from the edge of the optic nerve. One mouse was used as a nonlasered control for visualization of normal choroid–RPE structure (Supplementary Fig. S1).

### Drugs and Treatment

Mice were divided into three groups: minocycline, DAM, and control ( $n = 4$  males, 4 females per group). Minocycline HCl (Sigma-Aldrich, St. Louis, MO, USA, catalog no. 13614-98-7) and DAM HCl (>98% purity, structure confirmed by Liquid Chromatography-Mass Spectrometry (LCMS) and Nuclear Magnetic Resonance (NMR), created by MS, and purchased from AttachChem, Lubbock, TX, USA) were dissolved and suspended, respectively, in sterile saline (0.9% NaCl in water) to a concentration of 10 mg/mL. Sterile saline (0.9% NaCl in water) was used for controls. All treatments were administered bilaterally via topical eye drops twice a day for 2 weeks, starting the day after laser surgeries (see Fig. 1). Drops were left in each eye for 20 seconds while mice were firmly scruffed to allow time for absorption and to prevent nasal and/or oral ingestion of drops.

### Enucleation and Dissection of Eyes

Mice were humanely euthanized via carbon dioxide inhalation and cervical dislocation. Mice were decap-

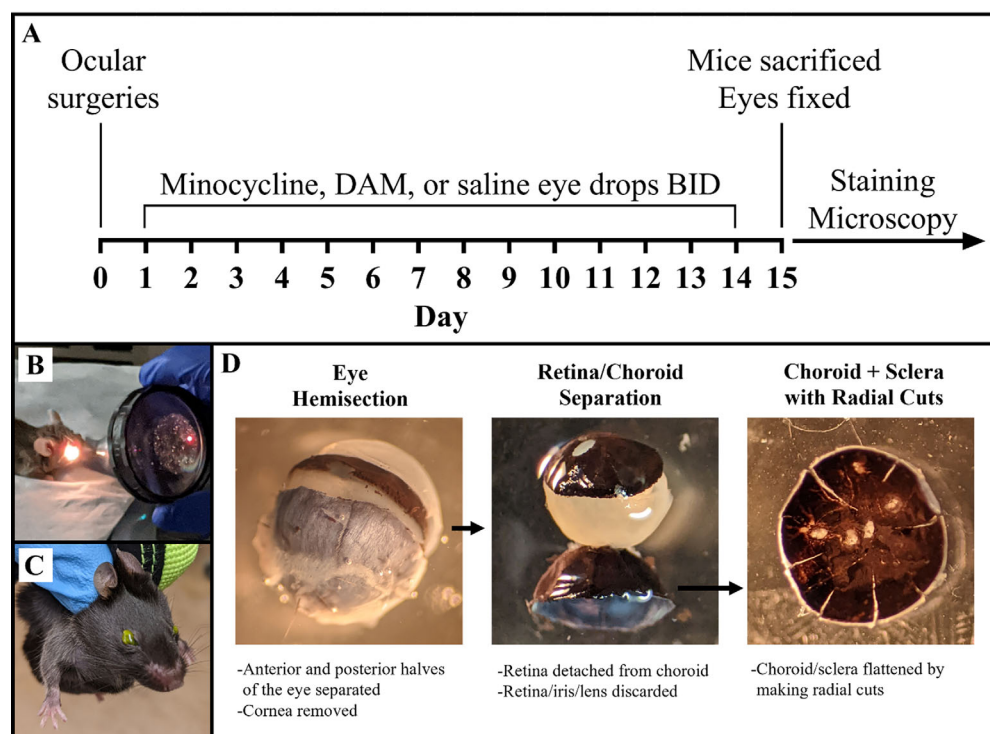


**Figure 1.** Experimental timeline and methods. **(A)** Timeline of ocular laser surgeries, drug treatments, dissections, immunohistochemistry, and confocal microscopy. **(B)** Laser disruption of Bruch's membrane to induce CNV formation. **(C)** Topical eye drop administration technique. **(D)** Enucleation and dissection of eyes: eyes were hemisected to separate anterior and posterior halves, retina was separated from underlying choroid, and radial cuts were made to facilitate flattening of samples for staining, flat mounting, and microscopy.

itated and a longitudinal fracture was placed along the dorsum of the skull. Tissue was dissected away to expose the orbital bones, which were cracked, taking care to avoid damaging the eyes. The optic nerve and extraocular muscles were severed. Once free, eyes were immediately fixed for 60 minutes in 4% paraformaldehyde in 1× phosphate-buffered saline (PBS; 9 g/L NaCl, 0.232 g/L  $\text{KH}_2\text{PO}_4$ , 0.703 g/L  $\text{Na}_2\text{HPO}_4$ ) (Invitrogen; Thermo Fisher Scientific, Waltham, MA, USA). Eyes were transferred to 1× PBS for further dissection. Eyes were hemisected using microsurgery scissors and fine tweezers to separate the anterior and posterior halves of the eyes. The crystalline lens and vitreous humor were removed. Retinas were separated from the underlying choroid/sclera eye cups. Radial cuts were made in the choroidal sections to allow them to flatten when mounted (see Fig. 1).

### Choroidal Flat Mounts

A solution of three fluorescent dyes was prepared: 4',6-diamidino-2-phenylindole (DAPI) (1:1:000 dilution of a 10 mg/mL solution), isolectin IB4 (1:100 dilution of a 1  $\mu\text{g}/\mu\text{L}$  solution, conjugated with Alexa Fluor 568), and phalloidin (1:100 dilution of a 0.2 U/ $\mu\text{L}$  solution, conjugated with Alexa Fluor

488) (Invitrogen, Waltham, MA, USA). Fluorescent signals for DAPI (405 nm, blue), phalloidin (488 nm, green), and isolectin IB4 (568 nm, red) were used to visualize nuclei, RPE, and blood vessels, respectively. Choroid/sclera eye cups were washed with cold Immunocytochemistry (ICC) buffer (0.5% bovine serum albumin, 0.2% Tween 20, 0.05% sodium azide) in 1× PBS (9 g/L NaCl, 0.232 g/L  $\text{KH}_2\text{PO}_4$ , 0.703 g/L  $\text{Na}_2\text{HPO}_4$  [pH 7.3]), then incubated with the fluorescent dyes at 4°C with gentle rotation for 4 hours in a humidified chamber. After incubation, choroid/sclera eye cups were washed by placing them briefly in a 1 mL solution of cold ICC buffer, then flat-mounted, covered, and sealed.

### CNV Evaluation and Quantification

CNV complexes were visualized using a Nikon Ti-E inverted microscope with A1 confocal module (Nikon, Melville, NY, USA). Horizontal optical sections were collected from the surface of the RPE/choroid/sclera complexes to a depth at which choroidal vascular networks could no longer be observed. All images were taken at 20× magnification at 1024 × 1024-pixel resolution and at a depth of 8 bits per channel. All lesions were imaged and evaluated for each mouse.

CNV burn lesions were excluded from analysis if an error occurred during laser surgeries (one lesion), if lesions were damaged during eye removal or dissection (six lesions), if two lesions merged as a result of being placed too close together (four lesions), or if a major non-CNV vessel crossed the lesion (one lesion).

CNV volumes were quantified in cubic micrometers as previously described,<sup>39,40</sup> with the exceptions that NIS-Elements Imaging Software (Nikon) was used for analysis and non-CNV blood vessels on the periphery of microscopy frames were excluded from analysis. Images of individual cross sections were saved as confocal ND2 files and used to generate three-dimensional reconstructions of each CNV complex. All settings were kept constant across all images. The red channel (TRITC, isolectin IB4) was used to identify CNV complexes. All three channels (blue, DAPI, nuclei; green, FITC, RPE; and red, TRITC, blood vessels) were used to draw a Bezier region of interest for each lesion to exclude any blood vessels outside the diameter of the lesions. A conservative intensity threshold for the red channel was used to exclude any background signal. The summation of fluorescent area within the Bezier regions of interest within each horizontal section was used as an index for CNV volume. All imaging and analyses were carried out by an individual blinded to treatment groups.

Results of the volume measurements were analyzed with Prism version 7.00 (GraphPad Software, San Diego, CA, USA). CNV volumes were averaged across all burns for each mouse. CNV volumes were expressed as mean  $\pm$  SEM. Two-way analyses of variance (ANOVAs) with Tukey's multiple comparisons test were used to determine any differences in CNV volume between treatment groups and between female and male mice. A one-way ANOVA with Bonferroni's multiple comparisons test was used to analyze differences between control, minocycline, and DAM treatment groups with data from male and female mice combined.

## Antimicrobial Activity of Minocycline and DAM

Antimicrobial testing was conducted as previously described.<sup>42,43</sup> To compare the antimicrobial action of DAM to minocycline, zone of inhibition (ZOI) assays were conducted for *Escherichia coli* and colony-forming unit (CFU) assays were performed using *E. coli* and *Candida albicans* as a representative of bactericidal and fungicidal activity, respectively. In the ZOI assays, we used the disc diffusion testing method for our experiments as previously described.<sup>44,45</sup> The disc diffusion testing method and CFU assay are well-

standardized, reliable susceptibility testing techniques. Briefly, bacteria were grown overnight in LB medium. The following day, the bacterial culture was washed in Mueller Hinton (MH) broth (#70192; Sigma-Aldrich), and the bacterial suspension was adjusted to an OD<sub>600</sub> of 0.1 (which is equivalent to the 0.5 McFarland standard;  $\sim 1 \times 10^7$  bacterial cell/mL) in MH broth according to the standard guidelines of the National Committee for Clinical Laboratory Standards.<sup>44,45</sup> Following this, a sterile cotton swab was dipped into the adjusted bacterial culture, and a lawn of bacteria was spread on an LB Agar plate. The test discs were prepared by adding 20  $\mu$ L DAM, minocycline, or sterile water solutions onto 6 mm diameter blank BD BBL Sensi-Disc Antimicrobial Susceptibility Test Discs (#B31039; Fisher Scientific, Waltham, MA, USA). Triplicate discs were distributed evenly onto the LB Agar surface. The plates were then incubated at 37°C for 24 hours before the results were read and recorded. The diameters of the zones of complete and clear inhibition, including the diameter of the disc, were measured to the nearest millimeter with a caliper.

To determine the minimum fungicidal concentration of DAM using the CFU assay, *C. albicans* (ATCC 3147, Pamela Parr) was grown in Yeast Peptone Dextrose (YPD) broth at 35°C for 48 hours. Aliquots of the 48 hour cultures were inoculated into fresh YPD broth to an OD<sub>600</sub>  $\sim 1.00$ . DAM was diluted in YPD broth at concentrations of 10, 25, 50, or 100  $\mu$ g/mL and 1 mL aliquots of each were pipetted in triplicate into the wells of a 24 microtiter well plate. The wells were inoculated using 10  $\mu$ L aliquots of the adjusted cultures for an initial inoculum of  $10^5$  CFU/mL and the microtiter well plates were incubated at 35°C. After 24 hours of incubation, the cultures were serially diluted 10-fold, plated on YPD agar, and incubated at 35°C for 24 hours to quantify the CFU/mL present.

## Inhibition of MMPs by DAM and Minocycline

MMP-9 inhibition was tested using a dose response of 0, 25, 50, and 75  $\mu$ M minocycline and DAM using the Abcam assay (AB284517; Abcam, Waltham, MA, USA).

## Results

### Minocycline and DAM Inhibit Experimental Choroidal Neovascularization

Treatment with minocycline significantly reduced CNV lesion volume in both female and male mice ( $F_{1,12} = 15.2$ ,  $P = 0.0021$ ) (Fig. 2A, Fig. 3, Fig. 4, Supplemental Fig. S2). Treatment worked equally well



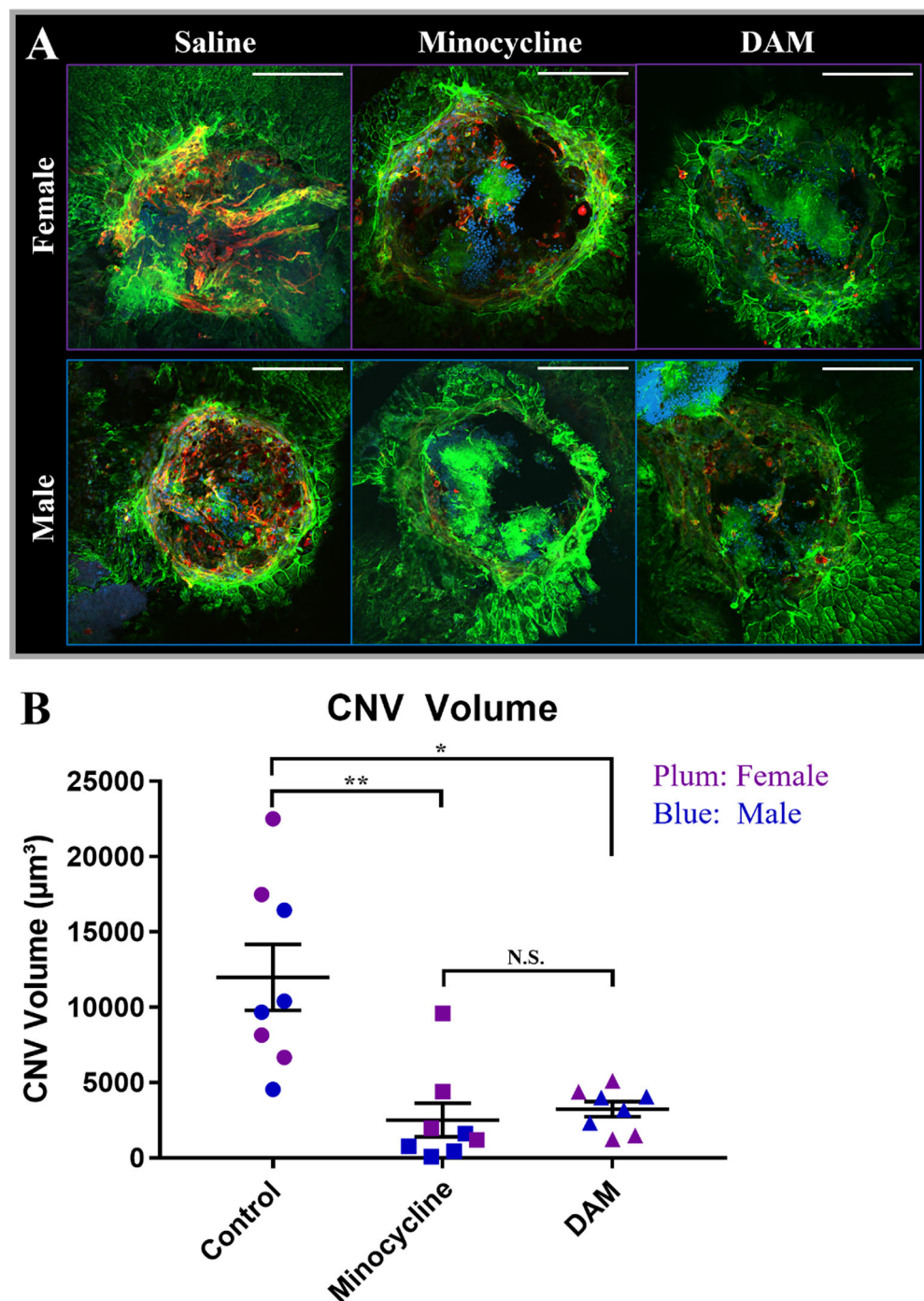


**Figure 2.** Minocycline and DAM eye drops reduce CNV volume in female and male mice. **(A)** Representative images of CNV lesions in mice treated with saline ( $n = 4$  females and 4 males), minocycline ( $n = 4$  females and 4 males), or DAM ( $n = 4$  females and 4 males) for 2 weeks. Lesions were labeled with fluorescent markers for isolectin IB4 (red; blood vessels), phalloidin (green; RPE), and DAPI (blue; nuclei). All settings were kept constant across all images, for both confocal microscopy and image analysis. Scale bar: 100  $\mu\text{m}$ . **(B)** Plot of CNV lesion volumes in saline, minocycline, and DAM treatment groups. Each point corresponds to the average volume of CNV lesions in both left and right eyes of a single mouse. A one-way ANOVA with Bonferroni's multiple comparisons test was used to analyze differences between control, minocycline, and DAM treatment groups with data from male and female mice combined.  $*P < 0.0005$ ,  $**P < 0.001$ . Error bars represent standard error of the mean.

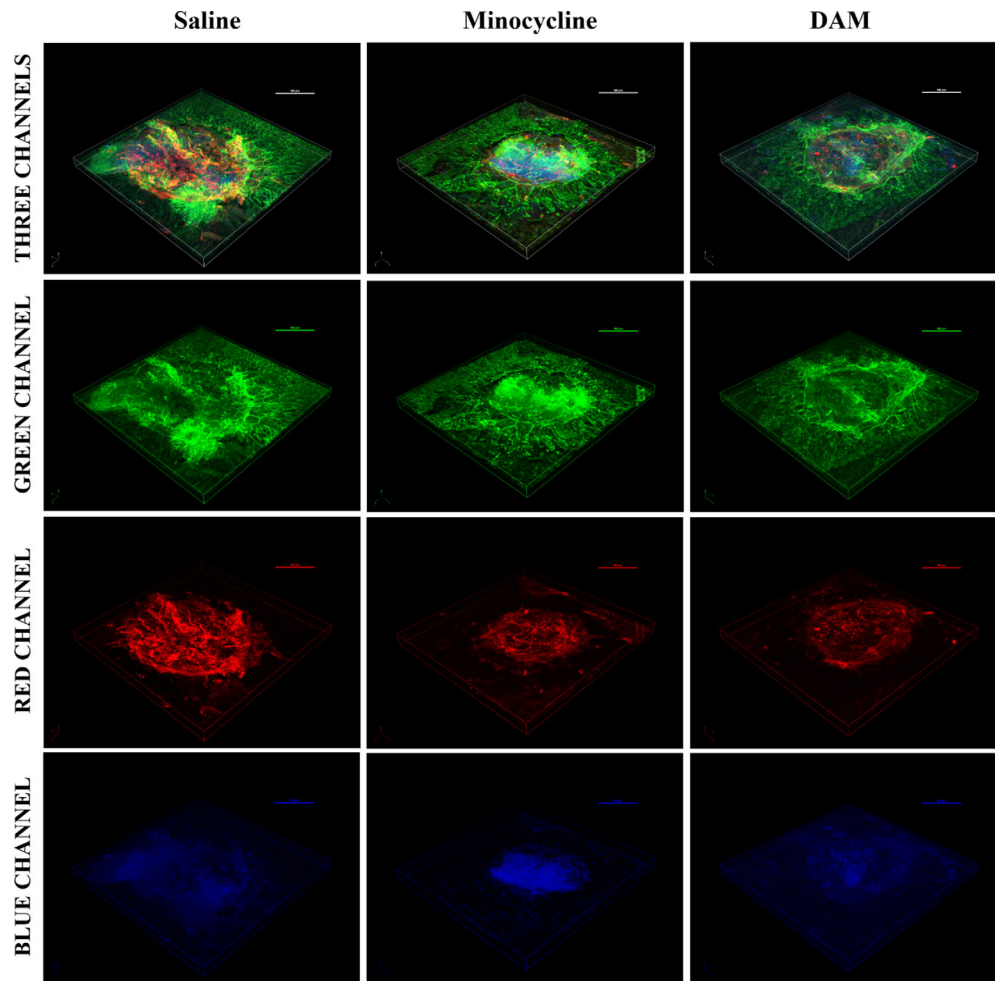


**Figure 3.** Representative three-dimensional reconstructions of CNV lesions in female mice. Mice were treated with saline ( $n = 4$  females and 4 males), minocycline ( $n = 4$  females and 4 males), or DAM ( $n = 4$  females and 4 males) eye drops for 2 weeks. All settings were kept constant across all images, for both confocal microscopy and image analysis. Scale bar: 100  $\mu\text{m}$ . Three channels: green (RPE), red (blood vessels), and blue (nuclei) channels superimposed. Green channel: phalloidin-labeled RPE. Red channel: isolectin IB4-labeled blood vessels. Blue channel: DAPI-labeled nuclei.

between sexes as there was no significant difference in CNV volume between female and male mice ( $F_{1,12} = 2.026$ ,  $P = 0.1801$ ). Treatment with DAM also significantly reduced CNV lesion volume in both female and male mice ( $F_{1,12} = 14.54$ ,  $P = 0.0025$ ) (Fig. 2A, Fig. 3, Fig. 4, Supplemental Fig. S2). Again, DAM treatment worked equally well in female and male mice as there was no significant difference in CNV volume ( $F_{1,12} = 0.4373$ ,  $P = 0.5209$ ) and no drug  $\times$  sex interaction.

Because sex did not have a significant impact on CNV volume between control and minocycline or control and DAM treatment groups, the data from female and male mice were combined and further evaluated. Treatment with minocycline reduced CNV lesion volume by 79% compared to control ( $P = 0.0004$ ; 95% confidence interval [CI], 4212–

14,792) (Fig. 2, Fig. 3, Fig. 4). Treatment with DAM reduced CNV lesion volume by 73% compared to control ( $P = 0.0009$ ; 95% CI, 3493–14,074) (Fig. 2, Fig. 3, Fig. 4). Both minocycline and DAM worked equally well as there was no significant difference between treatment groups ( $n = 8$ ,  $P > 0.9999$ ) (Fig. 2, Fig. 3, Fig. 4).

### Antimicrobial Activity of Minocycline and DAM

DAM had no antibacterial activity against *E. coli* at doses 400 times higher than the antibacterial dose of minocycline (Fig. 5). DAM had no antifungal activity against *C. albicans* at doses twice the antifungal dose of minocycline (Fig. 5).

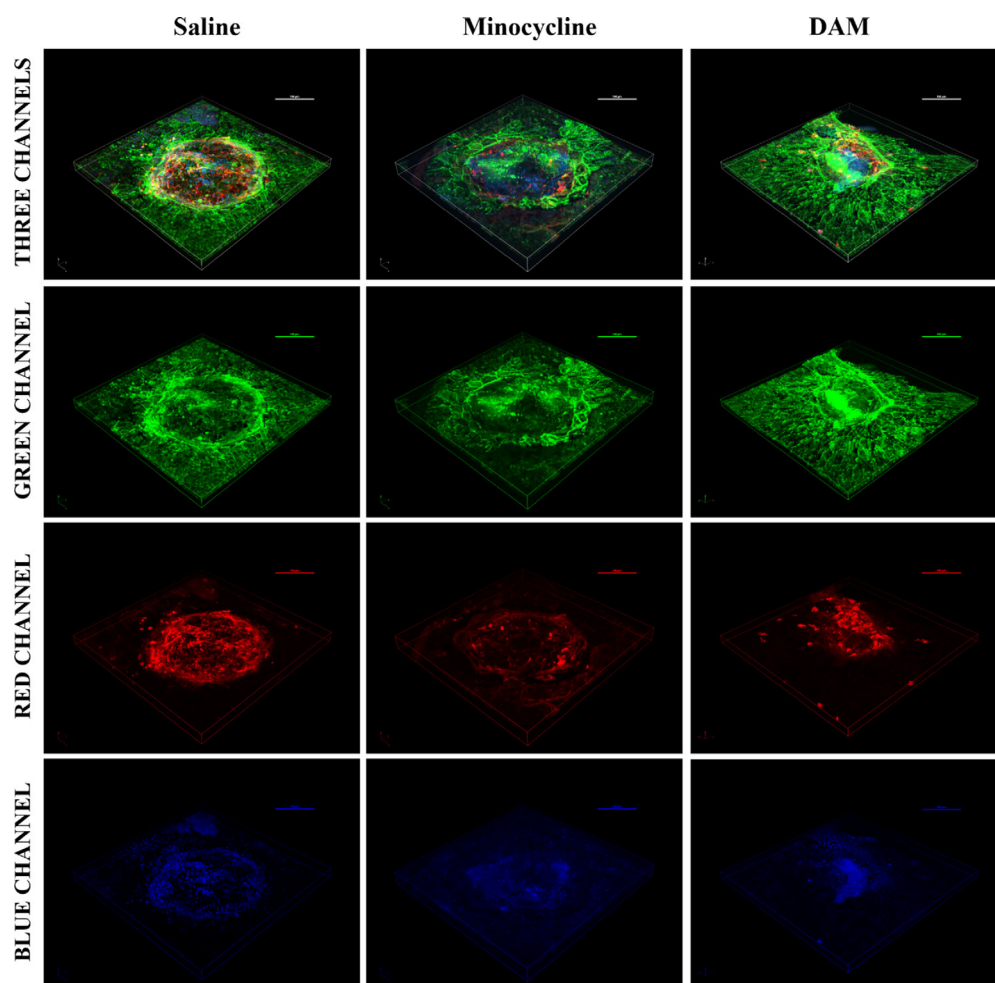


**Figure 4.** Representative three-dimensional reconstructions of CNV lesions in male mice. Mice were treated with saline ( $n = 4$  females and 4 males), minocycline ( $n = 4$  females and 4 males), or DAM ( $n = 4$  females and 4 males) eye drops for 2 weeks. All settings were kept constant across all images, for both confocal microscopy and image analysis. Scale bar: 100  $\mu\text{m}$ . Three channels: green (RPE), red (blood vessels), and blue (nuclei) channels superimposed. Green channel: phalloidin-labeled RPE. Red channel: isolectin IB4-labeled blood vessels. Blue channel: DAPI-labeled nuclei.

## MMP Inhibition by Minocycline and DAM

Both minocycline and DAM showed inhibition of MMP, with DAM showing stronger inhibition at lower doses (see Supplemental Fig. 3).

## Discussion

Pathologic CNV is a major cause of significant vision loss. Previously, Cox et al.<sup>40</sup> showed that oral doxycycline reduced pathologic angiogenesis in a laser-induced model of CNV in mice. Further studies have shown that oral minocycline, another tetracycline derivative, inhibits retinal neovascularization.<sup>23,24</sup> On the basis of those findings, we tested minocycline and DAM eye drops for efficacy to reduce

pathologic angiogenesis. Consistent with other ocular studies, we found that minocycline and DAM eye drops significantly reduced CNV lesion volume compared to control. Importantly, we found treatments worked equally well in both sexes, something that had not been previously tested preclinically. The success of tetracycline analogues in ocular neovascular disorders<sup>23,40,46–48</sup> has translated to promising outcomes in clinical trials. A phase I/II clinical trial (NCT01120899) found that oral minocycline (100 mg, twice a day for 6 months) improved visual function, central macular edema, and vascular leakage in patients with fovea-involving diabetic macular edema.<sup>29</sup> Another clinical trial (NCT00511875) found that oral doxycycline (50 mg, once daily for 24 months) improved inner retinal function in patients with severe nonproliferative diabetic retinopathy or non-high-risk proliferative

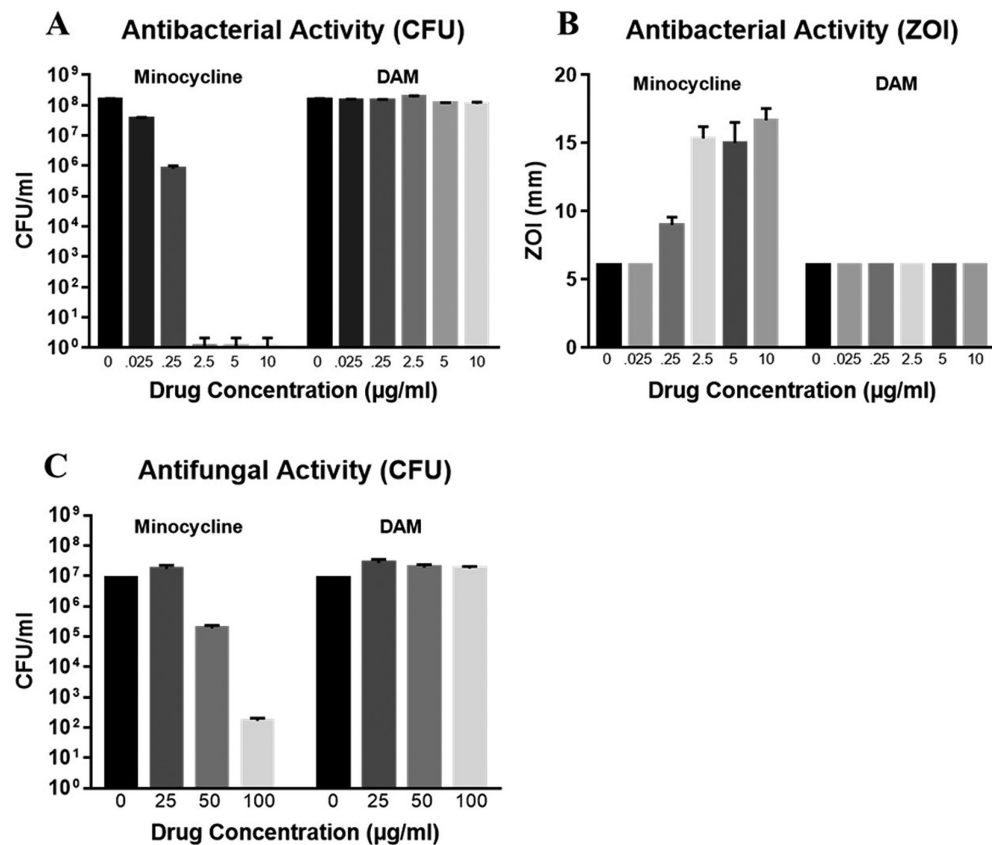


**Figure 5.** Antimicrobial activity of minocycline and DAM. **(A)** CFU assays to determine antibacterial activity of minocycline and DAM. DAM exhibited no antibacterial activity against *E. coli* at concentrations up to 10 μg/mL. **(B)** Zone of inhibition assays to determine antibacterial activity of minocycline and DAM. DAM exhibited no antibacterial activity against *E. coli* at concentrations up to 10 μg/mL. **(C)** CFU assays to determine antifungal activity of minocycline and DAM. DAM exhibited no antifungal activity against *C. albicans* at concentrations up to 100 μg/mL. All experiments were repeated in triplicate. Error bars represent standard error of the mean.

erative diabetic retinopathy.<sup>49</sup> This finding was not replicated in a concurrent trial (NCT00917553) on mild to moderate nonproliferative diabetic retinopathy conducted by the same group.<sup>50</sup> Combination therapy with reduced-fluence photodynamic therapy, intravitreal ranibizumab, intravitreal dexamethasone, and oral minocycline was effective to maintain stable vision in neovascular age-related macular degeneration in a clinical trial in the United Kingdom.<sup>16</sup> A clinical trial (NCT02564978) testing oral minocycline in age-related macular degeneration is projected to complete in 2023. On the basis of this translational success of tetracycline derivatives from preclinical to clinical studies, as well as our preclinical findings, we argue that minocycline and DAM eye drops may represent promising new therapeutic strategies for ocular neovascular disorders. The potential for the clinical translation of our findings is strengthened further because we tested our compounds in both female and male mice and found similar results, suggesting all patients can be treated and will likely see similar efficacy.

Targeted delivery of drugs to the choroid and retina is challenging due to multiple anatomic and physiologic barriers.<sup>51</sup> Because of this, most studies testing tetracycline derivatives in ocular neovascular disorders have employed an oral route of administration. While systemic minocycline and doxycycline are generally well tolerated,<sup>26,29,49</sup> their antimicrobial action can disrupt the gut microbiome, induce gastrointestinal side effects, and contribute to antimicrobial resistance.<sup>26,36,38,52</sup> Therefore, we hypothesized that targeted administration of minocycline via topical eye drops would reduce CNV lesion volume but carry less risk for systemic effects. We further hypothesized that DAM, a modified minocycline analogue that lacks antimicrobial action, could further reduce these risks. To our knowledge, we are the first to evaluate the effectiveness of tetracycline derivatives in a model of ocular neovascular disorders when administered via topical eye drops.

Fluorescein angiography and optical coherence tomography are alternative methods that have been



used to evaluate pathologic neovascularization in rodents.<sup>35,39</sup> However, fluorescein angiography can show incompetent blood vessels, and nonperfused vessels cannot be visualized.<sup>39</sup> While optical coherence tomography is a suitable alternative and has been used in similar studies,<sup>35</sup> laser-induced CNV with immunostaining and confocal microscopy was selected because it allows for high-resolution visualization and quantification of microscopic, newly formed blood vessels.<sup>39,40</sup>

Little is known about the safety of targeted administration of minocycline to the eye. A case study in 2017 reported that a single intraocular injection of minocycline (50 µg/0.1 mL) was not toxic when used for the treatment of ocular pythiosis.<sup>53</sup> While two studies in rabbits reported potential side effects after intraocular injections of tetracyclines,<sup>54,55</sup> those studies did not administer tetracyclines via topical eye drops, and intraocular inflammatory responses are stronger in rabbits compared to adult humans.<sup>55</sup> The current standard therapies (intravitreal anti-VEGF injections) also carry similar risk factors.<sup>41,56</sup> Further, potential ocular side effects from topical minocycline can likely be mitigated through strategic delivery systems. For example, subconjunctival injection of minocycline encapsulated in nontoxic nanoliposomes successfully delivered drug to the retina, lens, cornea, and vitreous in rats and has the potential to reduce side effects.<sup>57</sup> The eye harbors a unique microbiome that may be disturbed by antibiotics such as minocycline.<sup>58,59</sup> DAM, which lacks antimicrobial action (Fig. 5), does not carry this risk.

While this study provides proof of concept that minocycline and DAM reduce CNV volume when administered topically via eye drops, our findings are limited in several ways. Laser-induced CNV is primarily applicable to pathologic processes that can take place in macular degeneration but does not model all aspects of macular degeneration or other CNV-related disorders. Laser injury may disrupt some of the barriers that could prevent drug delivery in nonlasered eyes. Further, there are major differences between topical delivery of ocular medications in mice compared to humans, a factor that has limited translatability of topical ocular medications in the past.<sup>60,61</sup> Further studies on the pharmacokinetics, pharmacodynamics, dosage, formulation, safety, tolerability, and mechanisms of minocycline and DAM eye drops are needed.

Nonetheless, the success of tetracycline analogues in preclinical studies as well as multiple clinical trials strengthens the potential of our findings. Our results show that minocycline and/or DAM eye drops are likely to increase effectiveness and patient satisfaction while lowering the overall treatment burden of current anti-VEGF injections used in treating vision-

threatening CNV. If effective in humans, both minocycline and DAM could lower the cost of treatment for CNV-related disorders compared to intravitreal injections because they would potentially require fewer serial or no injections. This could also decrease the overall treatment burden as patients' ophthalmology visits could decrease. The lack of need for a specialist to administer shots would also increase treatment accessibility, in terms of both financial cost as well as geographic location. Topical administration (as opposed to intravitreal injection) may reduce the risk for adverse events, such as endophthalmitis, infection, and eye irritation. Finally, a study by Chalam et al.<sup>62</sup> found that interleukin 6 levels correlate with resistance to anti-VEGF treatment in AMD, further increasing the need for alternative interventions. Taken together, topical minocycline and/or DAM eye drops may represent a promising new treatment strategy for CNV-related disorders.

## Acknowledgments

The authors thank Petar Grozdanov and the Texas Tech University Health Sciences Center Imaging Core for assistance with confocal microscopy and imaging analysis and Daniel Albert and David Wilson for their helpful advice on ocular anatomy, confocal microscopy image analysis, and sample preparation.

Supported by the Center for Translational Neuroscience and Therapeutics and the Department of Pharmacology and Neuroscience at Texas Tech University Health Sciences Center.

Disclosure: **J.O. Willms**, None; **K. Mitchell**, None; **M. Shashtri**, (E & P), AttachChem (E); **O. Sundin**, None; **X. Liu**, None; **P. Panthagani**, None; **P. Tran**, None; **S. Navarro**, None; **C. Sniegowski**, None; **A.A. Shaik**, None; **T. Chaudhury**, None; **T.W. Reid**, (P); **S.E. Bergeson**, (P)

\* JOW and KM contributed equally to this article.

## References

1. Gariano RF, Gardner TW. Retinal angiogenesis in development and disease. *Nature*. 2005;438(7070):960–966.
2. Green WR, Wilson DJ. Choroidal neovascularization. *Ophthalmology*. 1986;93(9):1169–1176.

3. Grossniklaus HE, Green WR. Choroidal neovascularization. *Am J Ophthalmol.* 2004;137(3):496–503.
4. Campochiaro PA. Seeing the light: new insights into the molecular pathogenesis of retinal diseases. *J Cell Physiol.* 2007;213(2):348–354.
5. Campochiaro PA; the First ARVO/Pfizer Institute Working Group. Ocular versus extraocular neovascularization: mirror images or vague resemblances. *Invest Ophthalmol Vis Sci.* 2006;47(2):462–474.
6. Kwak N, Okamoto N, Wood JM, Campochiaro PA. VEGF is major stimulator in model of choroidal neovascularization. *Invest Ophthalmol Vis Sci.* 2000;41(10):3158–3164.
7. Altmann C, Schmidt MHH. The role of microglia in diabetic retinopathy: inflammation, microvasculature defects and neurodegeneration. *Int J Mol Sci.* 2018;19(1):110.
8. Grigsby JG, Cardona SM, Pouw CE, et al. The role of microglia in diabetic retinopathy. *J Ophthalmol.* 2014;2014:705783.
9. Kowluru RA, Mishra M. Regulation of matrix metalloproteinase in the pathogenesis of diabetic retinopathy. In: Khalil RA, ed. *Progress in Molecular Biology and Translational Science.* Vol. 148. Matrix Metalloproteinases and Tissue Remodeling in Health and Disease: Target Tissues and Therapy. Academic Press; 2017:67–85.
10. Nussenblatt RB, Ferris F. Age-related macular degeneration and the immune response: implications for therapy. *Am J Ophthalmol.* 2007;144(4):618–626.e2.
11. Steen B, Sejersen S, Berglin L, Seregard S, Kvanta A. Matrix metalloproteinases and metalloproteinase inhibitors in choroidal neovascular membranes. *Invest Ophthalmol Vis Sci.* 1998;39(11):2194–2200.
12. Tatar O, Adam A, Shinoda K, et al. Matrix metalloproteinases in human choroidal neovascular membranes excised following verteporfin photodynamic therapy. *Br J Ophthalmol.* 2007;91(9):1183–1189.
13. Zeng H, WR Green, Tso MOM. Microglial activation in human diabetic retinopathy. *Arch Ophthalmol.* 2008;126(2):227–232.
14. Ma L, Dou HL, Wu YQ, et al. Lutein and zeaxanthin intake and the risk of age-related macular degeneration: a systematic review and meta-analysis. *Br J Nutr.* 2012;107(3):350–359.
15. Mitchell P, Liew G, Gopinath B, Wong TY. Age-related macular degeneration. *Lancet.* 2018;392(10153):1147–1159.
16. Sivaprasad S, Patra S, DaCosta J, et al. A pilot study on the combination treatment of reduced-fluence photodynamic therapy, intravitreal ranibizumab, intravitreal dexamethasone and oral minocycline for neovascular age-related macular degeneration. *Ophthalmologica.* 2011;225(4):200–206.
17. Stahl A. The diagnosis and treatment of age-related macular degeneration. *Dtsch Arztebl Int.* 2020;117(29–30):513–520.
18. Ueta T, Noda Y, Toyama T, Yamaguchi T, Amano S. Systemic vascular safety of ranibizumab for age-related macular degeneration: systematic review and meta-analysis of randomized trials. *Ophthalmology.* 2014;121(11):2193–2203.e1–7.
19. Obeid A, Gao X, Ali FS, et al. Loss to follow-up among patients with neovascular age-related macular degeneration who received intravitreal anti-vascular endothelial growth factor injections. *JAMA Ophthalmol.* 2018;136(11):1251–1259.
20. Patel S. Medicare spending on anti-vascular endothelial growth factor medications. *Ophthalmol Retina.* 2018;2(8):785–791.
21. Jung HJ, Seo I, Jha BK, Suh SI, Suh MH, Baek WK. Minocycline inhibits angiogenesis in vitro through the translational suppression of HIF-1 $\alpha$ . *Arch Biochem Biophys.* 2014;545:74–82.
22. Yao JS, Shen F, Young WL, Yang GY. Comparison of doxycycline and minocycline in the inhibition of VEGF-induced smooth muscle cell migration. *Neurochem Int.* 2007;50(3):524–530.
23. Wu Y, Chen Y, Wu Q, Jia L, Du X. Minocycline inhibits PARP-1 expression and decreases apoptosis in diabetic retinopathy. *Mol Med Rep.* 2015;12(4):4887–4894.
24. Xu W, Yin J, Sun L, et al. Impact of minocycline on vascularization and visual function in an immature mouse model of ischemic retinopathy. *Sci Rep.* 2017;7(1):7535.
25. Xiao O, Xie Z-L, Lin B-W, Yin X-F, Pi R-B, Zhou S-Y. Minocycline inhibits alkali burn-induced corneal neovascularization in mice. *PLoS One.* 2012;7(7):e41858.
26. Garrido-Mesa N, Zarzuelo A, Gálvez J. Minocycline: far beyond an antibiotic. *Br J Pharmacol.* 2013;169(2):337–352.
27. Kim HS, Suh YH. Minocycline and neurodegenerative diseases. *Behav Brain Res.* 2009;196(2):168–179.
28. Stirling DP, Koochesfahani KM, Steeves JD, Tetzlaff W. Minocycline as a neuroprotective agent. *Neurosci Rev J Bringing Neurobiol Neurol Psychiatry.* 2005;11(4):308–322.

29. Cukras CA, Petrou P, Chew EY, Meyerle CB, Wong WT. Oral minocycline for the treatment of diabetic macular edema (DME): results of a phase I/II clinical study. *Invest Ophthalmol Vis Sci*. 2012;53(7):3865–3874.
30. Mirshahi A, Azimi P, Abdolahi A, Mirshahi R, Abdollahian M. Oral doxycycline reduces the total number of intraocular bevacizumab injections needed to control neovascular age-related macular degeneration. *Med Hypothesis Discov Innov Ophthalmol J*. 2017;6(2):23–29.
31. Zhao L, Ma W, Fariss RN, Wong WT. Minocycline attenuates photoreceptor degeneration in a mouse model of subretinal hemorrhage. *Am J Pathol*. 2011;179(3):1265–1277.
32. Peng X, Xiao H, Tang M, et al. Mechanism of fibrosis inhibition in laser induced choroidal neovascularization by doxycycline. *Exp Eye Res*. 2018;176:88–97.
33. He L, Marneros AG. Doxycycline inhibits polarization of macrophages to the proangiogenic M2-type and subsequent neovascularization. *J Biol Chem*. 2014;289(12):8019–8028.
34. Samtani S, Amaral J, Campos MM, Fariss RN, Becerra SP. Doxycycline-mediated inhibition of choroidal neovascularization. *Invest Ophthalmol Vis Sci*. 2009;50(11):5098–5106.
35. Li X, Zhang W, Ye Z, Pei S, Zheng D, Zhu L. Safety evaluation and pharmacodynamics of minocycline hydrochloride eye drops. *Mol Vis*. 2022;28:460–479.
36. Schmidtner AK, Slattery DA, Gläsner J, et al. Minocycline alters behavior, microglia and the gut microbiome in a trait-anxiety-dependent manner. *Transl Psychiatry*. 2019;9(1):1–12.
37. Chopra I, Roberts M. Tetracycline antibiotics: mode of action, applications, molecular biology, and epidemiology of bacterial resistance. *Microbiol Mol Biol Rev*. 2001;65(2):232–260.
38. Leigh SJ, Kaakoush NO, Westbrook RF, Morris MJ. Minocycline-induced microbiome alterations predict cafeteria diet-induced spatial recognition memory impairments in rats. *Transl Psychiatry*. 2020;10(1):1–13.
39. Campos M, Amaral J, Becerra SP, Fariss RN. A novel imaging technique for experimental choroidal neovascularization. *Invest Ophthalmol Vis Sci*. 2006;47(12):5163–5170.
40. Cox CA, Amaral J, Salloum R, et al. Doxycycline's effect on ocular angiogenesis: an in vivo analysis. *Ophthalmology*. 2010;117(9):1782–1791.
41. Mizutani T, Ashikari M, Tokoro M, Nozaki M, Ogura Y. Suppression of laser-induced choroidal neovascularization by a CCR3 antagonist. *Invest Ophthalmol Vis Sci*. 2013;54(2):1564–1572.
42. Alastruey-Izquierdo A, Melhem MSC, Bonfietti LX, Rodriguez-Tudela JL. Susceptibility test for fungi: clinical and laboratorial correlations in medical mycology. *Rev Inst Med Trop Sao Paulo*. 2015;57(suppl 19):57–64.
43. Bertout S, Dunyach C, Drakulovski P, Reynes J, Mallié M. Comparison of the Sensititre YeastOne dilution method with the Clinical Laboratory Standards Institute (CLSI) M27-A3 microbroth dilution reference method for determining MIC of eight antifungal agents on 102 yeast strains. *Pathol Biol (Paris)*. 2011;59(1):48–51.
44. Patel JB, Clinical and Laboratory Standards Institute, eds. *Performance Standards for Antimicrobial Disk Susceptibility Test; Approved Standards*. 12th ed. Wayne, PA: Committee for Clinical Laboratory Standards; 2015.
45. Ghannoum MA, Clinical and Laboratory Standards Institute, eds. *Method for Antifungal Disk Diffusion Susceptibility Testing of Yeasts; Approved Guideline*. 2nd ed., replaces M44-A. Wayne, PA: Committee for Clinical Laboratory Standards; 2009.
46. Chen W, Zhao M, Zhao S, et al. Activation of the TXNIP/NLRP3 inflammasome pathway contributes to inflammation in diabetic retinopathy: a novel inhibitory effect of minocycline. *Inflamm Res*. 2017;66(2):157–166.
47. Krady JK, Basu A, Allen CM, et al. Minocycline reduces proinflammatory cytokine expression, microglial activation, and caspase-3 activation in a rodent model of diabetic retinopathy. *Diabetes*. 2005;54(5):1559–1565.
48. Stieger K, Mendes-Madeira A, Meur GL, et al. Oral administration of doxycycline allows tight control of transgene expression: a key step towards gene therapy of retinal diseases. *Gene Ther*. 2007;14(23):1668–1673.
49. Scott IU, Jackson GR, Quillen DA, et al. Effect of doxycycline vs placebo on retinal function and diabetic retinopathy progression in patients with severe nonproliferative or non-high-risk proliferative diabetic retinopathy: a randomized clinical trial. *JAMA Ophthalmol*. 2014;132(5):535–543.
50. Scott IU, Jackson GR, Quillen DA, Klein R, Liao J, Gardner TW. Effect of doxycycline vs placebo on retinal function and diabetic retinopathy progression in mild to moderate nonproliferative diabetic retinopathy: a randomized proof-of-concept clinical trial. *JAMA Ophthalmol*. 2014;132(9):1137–1142.

51. Gote V, Sikder S, Sicotte J, Pal D. Ocular drug delivery: present innovations and future challenges. *J Pharmacol Exp Ther*. 2019;370(3):602–624.
52. Vaughn AC, Cooper EM, DiLorenzo PM, et al. Energy-dense diet triggers changes in gut microbiota, reorganization of gut-brain vagal communication and increases body fat accumulation. *Acta Neurobiol Exp (Warsz)*. 2017;77(1):18–30.
53. Ros Castellar F, Sobrino-Jiménez C, del-Hierro-Zarzuelo A, Herrero-Ambrosio A, Boto-de-los-Bueis A. Intraocular minocycline for the treatment of ocular pythiosis. *Am J Health Syst Pharm*. 2017;74(11):821–825.
54. Falavarjani KG, Pourhabibi A, Aghdam KA, et al. Determination of the toxicity of intravitreal minocycline in rabbit eyes. *Cutan Ocul Toxicol*. 2016;35(3):233–236.
55. Horozoglu F, Metan G, Sever O, et al. Intravitreal tigecycline treatment in experimental *Acinetobacter baumannii* endophthalmitis. *J Chemother Florence Italy*. 2012;24(2):101–106.
56. Saint-Geniez M, Maharaj ASR, Walshe TE, et al. Endogenous VEGF is required for visual function: evidence for a survival role on Müller cells and photoreceptors. *PloS One*. 2008;3(11):e3554.
57. Kaiser JM, Imai H, Haakenson JK, et al. Nanoliposomal minocycline for ocular drug delivery. *Nanomed Nanotechnol Biol Med*. 2013;9(1):130–140.
58. Ranjith K, Sharma S, Shivaji S. Microbes of the human eye: microbiome, antimicrobial resistance and biofilm formation. *Exp Eye Res*. 2021;205:108476.
59. Delbeke H, Younas S, Casteels I, Joossens M. Current knowledge on the human eye microbiome: a systematic review of available amplicon and metagenomic sequencing data. *Acta Ophthalmol (Copenh)*. 2021;99(1):16–25.
60. Urtti A. Challenges and obstacles of ocular pharmacokinetics and drug delivery. *Adv Drug Deliv Rev*. 2006;58(11):1131–1135.
61. Maurice D. Practical issues in intravitreal drug delivery. *J Ocul Pharmacol Ther*. 2001;17(4):393–401.
62. Chalam KV, Grover S, Balaiya S, Murthy RK. Aqueous interleukin-6 (IL-6) level is a marker for treatment resistance to bevacizumab in age-related macular degeneration—aqueous cytokines after bevacizumab. *Open J Ophthalmol*. 2014;2014:24–30.

## Supplementary Material

Supplementary Figure S2. Movies of choroid/RPE flat mounts two weeks post laser surgery. Movies were generated from confocal Z-series taken at intervals of 2  $\mu\text{m}$ . Movies begin in the subretinal space and end towards the choroid. (A) Female mice treated with saline ( $n = 4$ ), (B) female mice treated with minocycline ( $n = 4$ ), (C) female mice treated with DAM ( $n = 4$ ), (D) male mice treated with saline ( $n = 4$ ), (E) male mice treated with minocycline ( $n = 4$ ), and (F) male mice treated with DAM ( $n = 4$ ). Green: phalloidin-labeled RPE. Red: isolectin IB4-labeled blood vessels. Blue: DAPI-labeled nuclei. All settings were kept constant across all images, both for confocal microscopy and image analysis. Scale bar: 100  $\mu\text{m}$ .

**Supplementary Figure 2A**  
**Supplementary Figure 2B**  
**Supplementary Figure 2C**  
**Supplementary Figure 2D**  
**Supplementary Figure 2E**  
**Supplementary Figure 2F**